Interaction-Induced Partitioning and Magnetization Jumps in the Mixed-Spin Oxide FeTiO_{3}-Fe_{2}O_{3}

M. Charilaou, K. K. Sahu, S. Zhao, J. F. Löffler, and A. U. Gehring

Phys. Rev. Lett. **107**, 057202 — Published 27 July 2011

DOI: 10.1103/PhysRevLett.107.057202

Interaction-induced partitioning and magnetization jumps in mixed-spin oxide $FeTiO_3$–Fe_2O_3

M. Charilaou,[1,2,*] K. K. Sahu,[2] S. Zhao,[3] J. F. Löffler,[2] and A. U. Gehring[1]

[1]*ETH Zurich, Department of Earth Sciences,*
Institute of Geophysics, Sonneggstrasse 5, 8092 Zurich, Switzerland.
[2]*ETH Zurich, Department of Materials,*
Laboratory of Metal Physics and Technology,
Wolfgang-Pauli-Strasse 10, 8093 Zurich, Switzerland.
[3]*ETH Zurich, Department of Physics, Laboratory for Solid State Physics,*
Schafmattstrasse 16, 8093 Zurich, Switzerland.

Abstract

In this study we report jumps in the magnetic moment of the hemo-ilmenite solid solution (x)$FeTiO_3$–(1-x)Fe_2O_3 above Fe(III) percolation at low temperature ($T < 3$ K). The first jumps appear at 2.5 K, one at each side of the magnetization loop, and their number increases with decreasing temperature and reaches 5 at $T = 0.5$ K. The jumps occur after field reversal from a saturated state and are symmetrical in trigger-field and intensity with respect to the field axis. Moreover, an increase of the sample temperature by 2.8% at $T = 2.0$ K indicates the energy released after the ignition of the magnetization jump, as the spin-currents generated by the event are dissipated in the lattice. The magnetization jumps are further investigated by Monte-Carlo simulations, which show that theese effects are a result of magnetic interaction-induced partitioning on a sublattice level.

PACS numbers: 75.30.Et, 75.47.Lx, 75.50.Lk

Keywords: magnetization jump, symmetry breaking, hemo-ilmenite, magnetic frustration

Complex magnetic systems that exhibit frustration are a topic of long-standing debate [1–5]. A typical example of the manifestation of magnetic frustration is the spin-glass freezing caused by competing exchange interactions due to their geometry [6–8]. The complex scheme of interactions does not allow the system to reach a ground state, and the system remains trapped in local minima of the energy landscape [6, 9, 10]. Application of an external field can move the system from one minimum to another, whereby the transfer can be either smooth or abrupt, depending on the morphology of the energy landscape. Abrupt effects are manifested in the form of metamagnetic transitions [11–13], which are characterized by sudden changes in the spin structure and thus in the net magnetization. These metamagnetic transitions may appear as single events, such as the spin-glass symmetry breaking along the de Almeida-Thouless (AT) line [14], or as multiple antiferromagnetic spin-flop transitions [15]. Another special case in the context of such phenomena is the occurrence of jumps in the magnetic moment [16–18]. Magnetization jumps have been observed in several materials and have been attributed to various properties, such as cluster formation [19–21] or frustration due to doping [22].

Among the systems regarding frustrated magnetism, there is one solid solution with a natural equivalent: hemo-ilmenite (x)$FeTiO_3$–(1-x)Fe_2O_3. Members of this solid solution can be important magnetic carriers in the Earth's crust and they are likely to be important constituents of other planets. Compositions with $0.50 < x < 0.95$ exhibit ferrimagnetic ordering and spin-glass-like freezing for $0.6 < x < 0.95$ at temperatures below $T < 40$ K [23, 24]. The solid solution crystallizes in the $R\bar{3}$c and $R\bar{3}$ symmetry, depending on the quenching temperature [25]. In the $R\bar{3}$c symmetry all cations are distributed evenly on a honeycomb lattice, whereas in the $R\bar{3}$ symmetry Fe(II) and Ti(IV) cations are partitioned in alternating sublattices and Fe(III) are distributed evenly (see inset to Fig. 1). Such distribution of Fe(II) and Fe(III) in the lattice generates a complex scheme of interactions, which also explains the spin-glass-like behavior. Although spin-glass-like freezing has been investigated for both synthetic [23, 24, 26–29] and natural samples [30, 31], the Fe(II)–Fe(III) coupling mechanisms are still ambiguous. Moreover, the hemo-ilmenite system represents an excellent example of a mixed-spin magnetic system with quasi-random interactions, and can be used as a testbed to investigate coupling effects of mixed-spin states. Such coupling effects are enhanced in the absence of thermal fluctuations, i.e., at low temperature. In this study we therefore performed magnetization measurements of hemo-ilmenite solid solutions

with $x = 0.7$, 0.8, and 0.9 deep in the frustrated state at low temperature ($T < 3$ K). For the discussion, the composition $x = 0.8$ is presented.

The solid solutions were synthesized by means of solid oxide reaction of the end members at $T = 1400$ K for 48 hrs, and the structure was investigated by powder X-ray diffraction. Rietveld analysis of the diffraction patterns reveals a single-phase hemo-ilmenite solid solution with the $R\bar{3}$ symmetry for $x = 0.9$ and 0.8, and $R\bar{3}$c for $x = 0.7$. Magnetization curves were recorded in a temperature range between 0.5 K $< T <$ 3.00 K in a Quantum Design Physical Property Measurement System (PPMS) (for $T > 2.0$ K) and in a Magnetic Property Measurement System (MPMS) (for $T < 2.0$ K). In the PPMS the field-sweep rate was set to 10 Oe/s, whereas in the MPMS the field was stopped for each measurement with the SQUID. In addition, the *ac* susceptibility was measured in a temperature range from 10 K to 300 K in the PPMS at a frequency of 1 kHz and driving-field amplitude of $H_{ac} = 5$ Oe.

Measurement of the *ac* susceptibility (Fig. 1) indicates long-range ferrimagnetic ordering at $T_{\rm C}$ with a peak in both the in-phase $\chi'(T)$ and out-of-phase component $\chi''(T)$ of the susceptibility. The exact ordering point is defined at the onset of $\chi''(T)$ upon cooling where hysteretic effects appear [32]. The Curie temperature for this solid solution is $T_{\rm C} = 238(1)$ K, consistent with a composition of $x = 0.8$ [33]. Fitting the high-temperature evolution of the inverse susceptibility χ'^{-1} with the Curie-Weiss law provides a Curie constant $C = Ng^2\mu_{\rm B}^2 J(J+1)/3k_{\rm B} = 4.25$, which gives an effective spin of $S = 2.44$ (considering that $L = 0$), close to the expected value of 5/2 for Fe(III). From this observation the ferrimagnetic ordering can be attributed to Fe(III).

Below 200 K, both components of the susceptibility decrease with decreasing temperature, and below 50 K $\chi'(T)$ exhibits a pronounced decrease, whereas $\chi''(T)$ shows a peak at the freezing temperature $T_{\rm f}$. Below $T_{\rm f}$ both components of $\chi(T)$ decrease with decreasing temperature. In addition, $\chi''(T)$ increases linearly with increasing driving field H_{ac}, indicating the absence of domains [29].

Fig. 2 shows a measurement of the magnetic moment deep in the frustrated phase at $T = 2.5$ K, where for small external fields ($H < 3$ kOe) the magnetic moment increases linearly with the external field H. The linear behavior of the total magnetic moment with H indicates spin-glass-like symmetry. However, at a critical trigger field $H_{\rm cr} = 4.5$ kOe an abrupt jump in the magnetic moment, and thus a symmetry breaking, is seen. The jump is very sharp with a width of $h = \Delta H/H_{\rm cr} \approx 0.04$, and exhibits an intensity $I = \Delta m/m_{\rm S}$

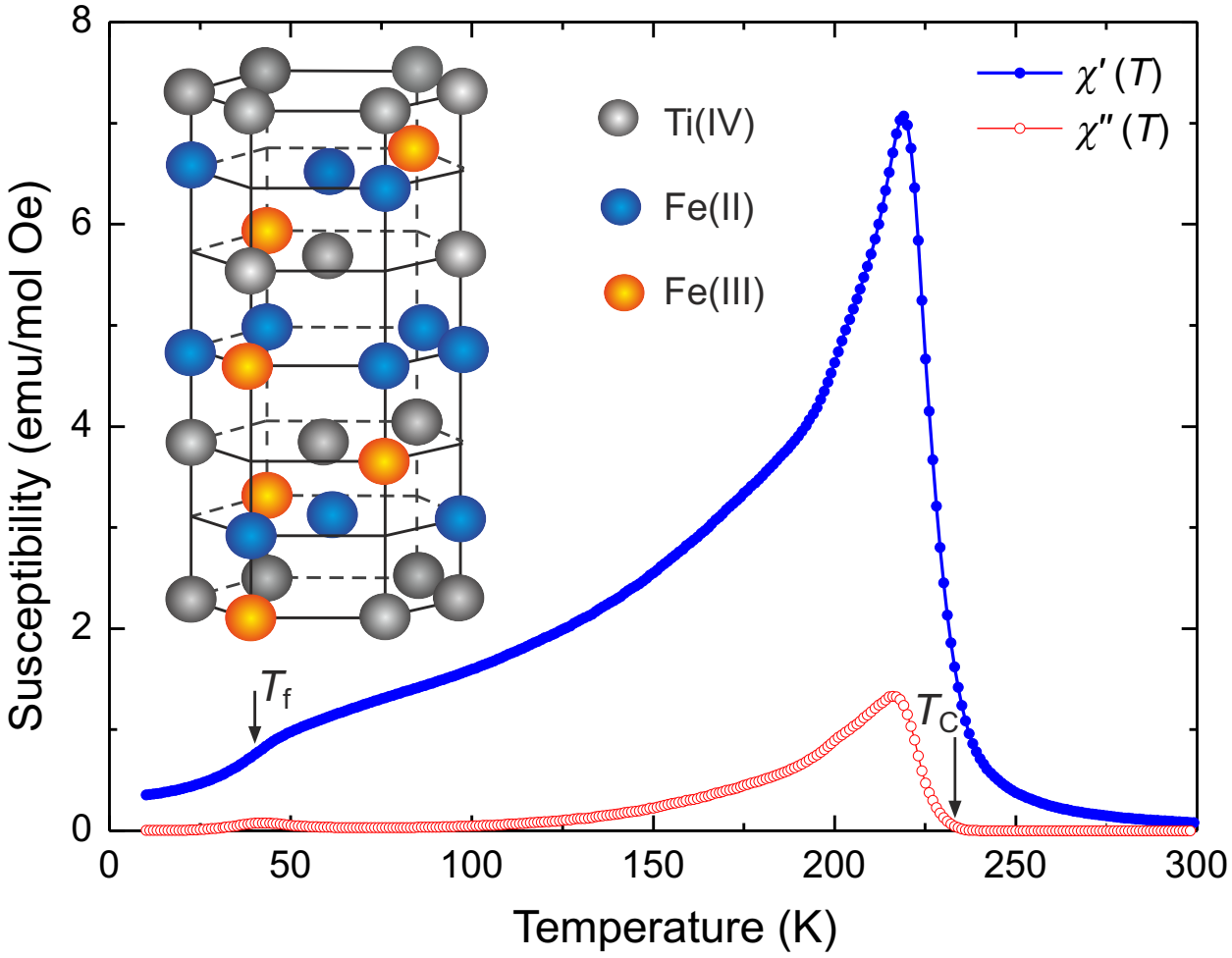

FIG. 1. Dynamic in-phase (full circles) and out-of-phase (open circles) *ac* susceptibility of the solid solution with $x = 0.8$ indicating the ferrimagnetic ordering at $T_{\rm C}$ and the spin-glass freezing at $T_{\rm f}$. The inset illustrates the cation ordering where the O(II) ions have been omitted.

of approximately 25%. After the jump the moment relaxes until the field catches up with the new state and then with increasing field the magnetic moment increases smoothly and reaches a pseudosaturation. While the field is reduced to zero the magnetic moment relaxes, again smoothly, and at $H = 0$ exhibits a relatively high remanence ($m/m_{\rm S} \approx 60\%$). The absence of a clear saturation can be attributed to crystallites with their c–axis perpendicular to the external field, because the layered $R\bar{3}$ structure requires spin alignment along c [34]. Nonetheless, we may define the saturation point to occurr at the collapse of the hysteresis loop, i.e., at $H \approx 20$ kOe.

The inset to Fig. 2 shows a comparison of full hysteresis loops at $T = 3.0$, i.e., above the

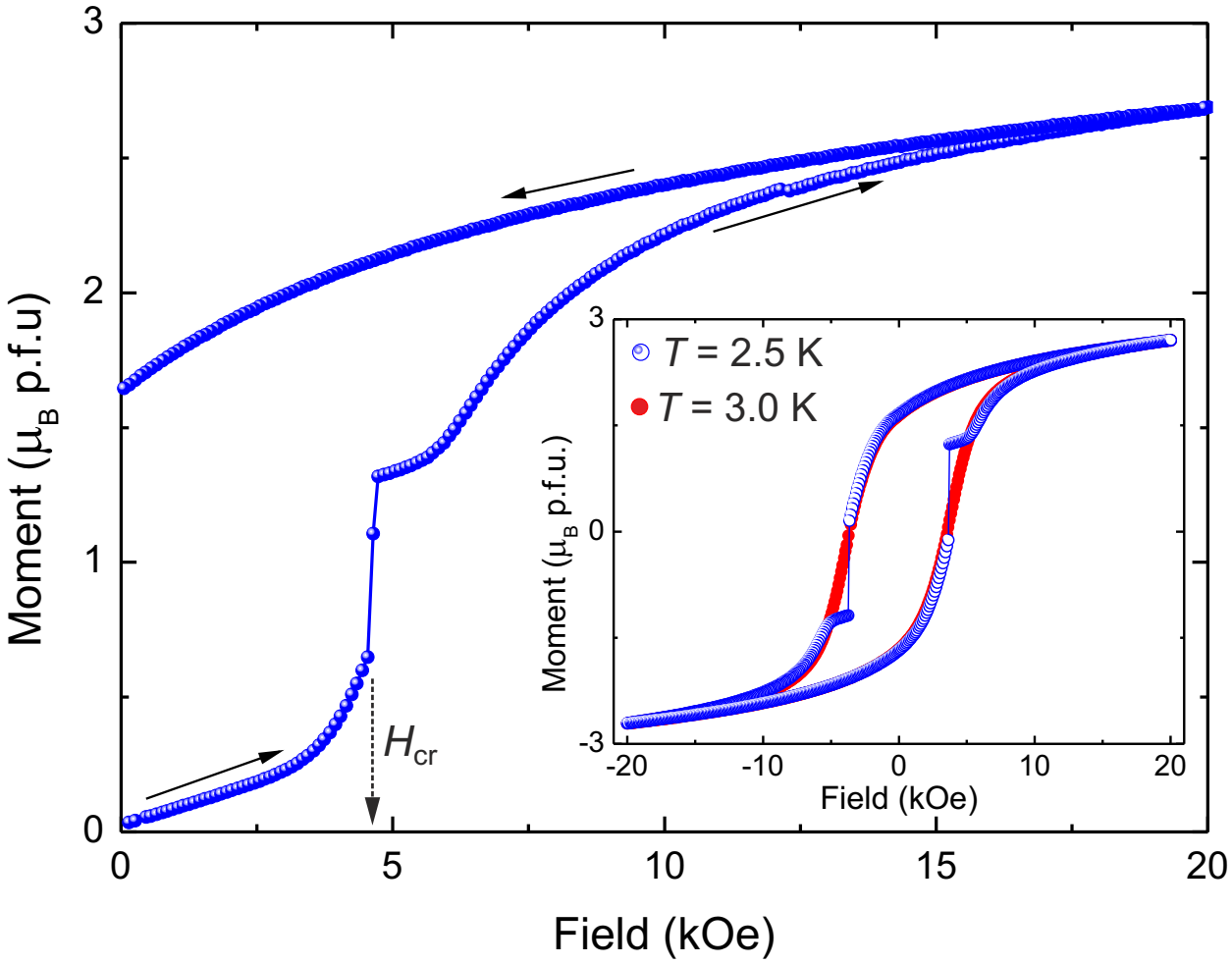

FIG. 2. Virgin line of the magnetization of solid solution with $x = 0.8$ at $T = 2.5$ K. The inset shows full hysteresis loops at $T = 2.5$ K (hollow spheres) and $T = 3.0$ K (full circles) for the same compound.

jump occurrence threshold, and at $T = 2.5$ K. At $T = 2.5$ K the hysteresis loop is almost identical to that at $T = 3$ K, apart from the fact that the reversal of the magnetization at $T = 2.5$ K occurs in a transition-like manner at the two critical trigger fields $\pm H_{\rm cr}$. The events are symmetrical in trigger field and amplitude ($I = \Delta m/m_{\rm S} \approx 50\%$) with respect to $H = 0$, and can be associated with the symmetry breaking observed in the virgin-line, after which the state with $m = 0$ is not favoured anymore. This suggests that the rapid re-arrangement of the magnetic structure is caused by the fact that the intermediate configurations (between $H = 3$ kOe and 5 kOe) cost energy.

With decreasing temperature the number of jumps increases and the total added intensity

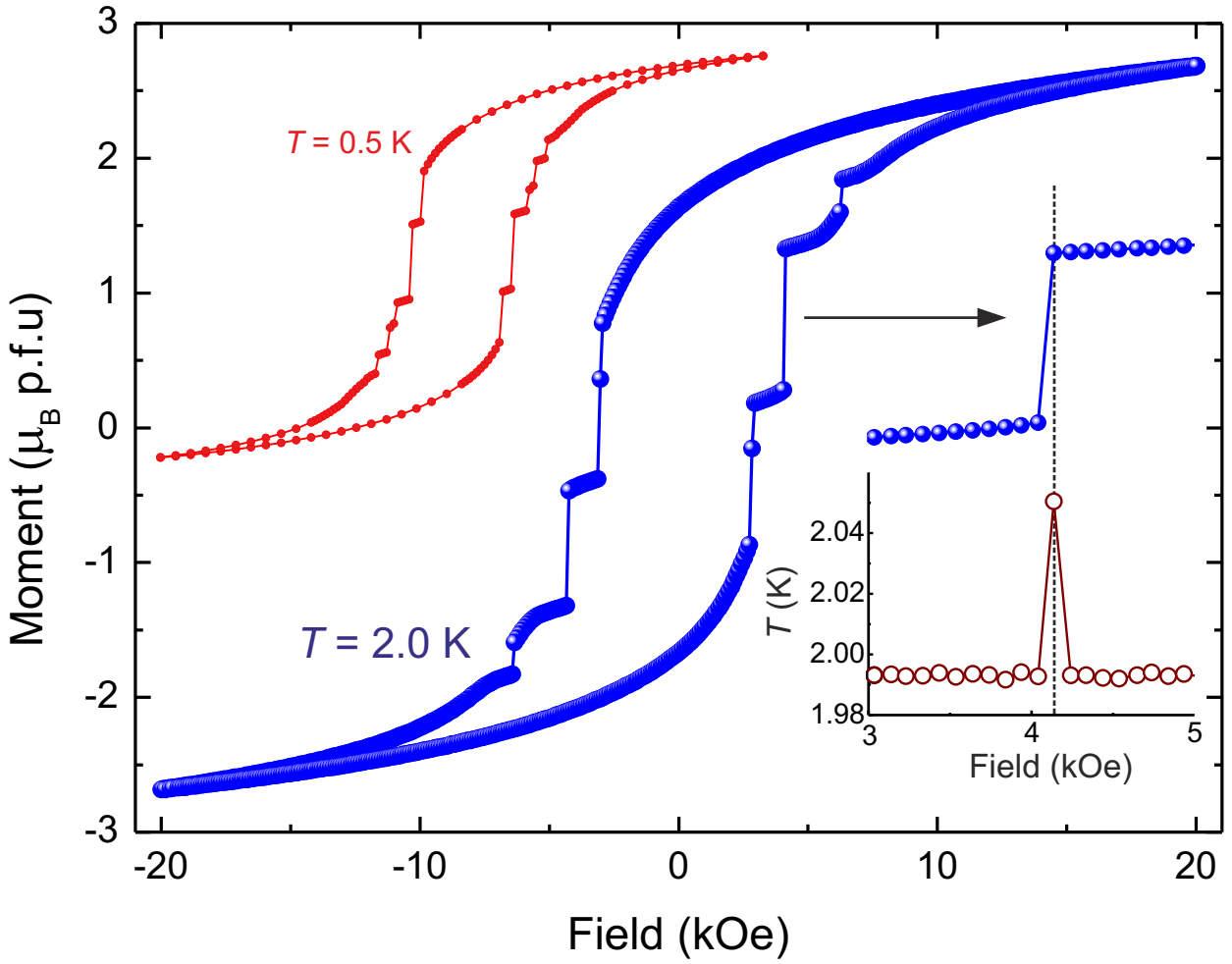

FIG. 3. Magnetization loop of solid solution with $x = 0.8$ at $T = 2.0$ K and blow-up of a jump illustrating temperature rise (lower right). Loop of same compound at $T = 0.5$ K (upper left), not to scale.

of the jumps becomes larger. At $T = 2.0$ K three and at $T = 0.5$ K five jumps on either side of the field axis are observed for solid solutions with $x = 0.8$ (Fig. 3 with inset). For solid solutions with $x = 0.9$ only two jumps were observed at $T = 2$ K: one large with $I \approx 35\%$ at $H_{\rm cr} = 4.6$ kOe and one small with $I \approx 6\%$ at $H_{\rm cr} = 8.5$ kOe (data not shown). These observations suggest that the number of magnetization jumps will most likely remain finite at zero-temperature.

In the inset of Fig. 3 a close-up of the most intense jump at $T = 2.0$ K and $H_{\rm cr} = 4.04$ kOe with intensity $I \approx 39\%$ is seen along with the sample temperature. At the critical field $H_{\rm cr}$ the magnetic moment jumps in a single motion (within the measurement time-frame of 10 s)

and then continues smoothly with increasing field. At the same time, the temperature shows a spike right after the event, with an increase of 2.8% from the base value of $T = 1.995$ K. This effect is a direct indicator of energy released by the magnetization jump, as the system reaches a new energy minimum. The actual energy released during the transition is in fact the difference in Zeemann energy $\Delta F_{\mathrm{Z}} = g\mu_{\mathrm{B}} HSI$ [16]. The measurable energy (heat), however, cannot be directly attributed to ΔF_{Z} but to its aftereffect. This aftereffect can be explained as follows: while the spin structure is rapidly re-arranging itself during the jump, the massive reversal results in pulses of spin-currents. These pulses are dissipated in the lattice, most likely, by means of eddy-currents, which then, in turn, become dissipated, and release heat.

Field-cooling experiments with various fields and field-sweep rate variation do not affect the occurrence or the features of the jumps. The hysteresis loops are reproducible with the same number of jumps and same properties, i.e. I and h, at each temperature. Therefore, we conclude that these effects are intrinsic to the system and are driven by processes on an atomic level, considering how sharp they appear in these powder samples. These phenomena occur, however, only for compositions close to, and above, the percolation threshold $x_p \approx 0.8$. We found magnetization jumps for $x = 0.9$ and $x = 0.8$ (both $R\bar{3}$), but not for $x = 0.7$ ($R\bar{3}$c). This further suggests atomic-scale processes governed by bond-percolation constraints [19, 20], because in the $R\bar{3}$ symmetry there is clear distinction between Fe-rich and Fe-deficient sublattices, as opposed to the $R\bar{3}$c symmetry. Hence, the occurrence of magnetization jumps can be attributed to collective sublattice reversal, whereas large jumps correspond to Fe-rich sublattices and small jumps correspond to Fe-deficient sublattices.

In order to test this scenario, we performed Monte-Carlo (MC) simulations using the Ising-like Hamiltonian

$$\mathcal{H} = -\frac{1}{2}\sum_{i,j} J_{\mathrm{ij}} S_i S_j - H\sum_i g_i S_i, \tag{1}$$

where J_{ij} is the exchange constant between the spins S_i and S_j and g_i the corresponding spectroscopic splitting factor, and H the external field. The spins take the values $\pm 4/2$ (Fe(II) – $3d^6$) and $\pm 5/2$ (Fe(III) – $3d^5$), whereas g is taken to be 1.5 for Fe(II) and 2.0 for Fe(III).

The presence of the two valence states of Fe requires three different exchange constants, i.e., $J_{\alpha\alpha}$ for Fe(II)–Fe(II), $J_{\beta\beta}$ for Fe(III)–Fe(III), and $J_{\alpha\beta}$ for Fe(II)–Fe(III) interactions,

whereas we assume isotropy ($J_{\alpha\beta} = J_{\beta\alpha}$). The energy and the field used in the calculations are scaled to $J_{\alpha\alpha}$. Considering the ordering temperature of the end-members (950 K for Fe_2O_3 and 58 K for $FeTiO_3$), and the respective number of nearest neighbors, a first estimate for the Fe(III)–Fe(III) interaction energy yields $J_{\beta\beta} \approx 5.7 \times J_{\alpha\alpha}$. In addition, $J_{\alpha\beta}$ can be estimated in a first approximation using mean field theory (MFT) predictions for the ordering temperature of a two-sublattice system by considering the known ordering temperature of the solid solution with composition $x = 0.66$, where Fe(II) and Fe(III) are in equal parts (T_C = 360 K). This results in $J_{\alpha\beta} = 2.3 \times J_{\alpha\alpha}$. In general, the coupling is governed by exchange and superexchange interactions along the c–axis. However, although the modulation length of $J_{\alpha\alpha}$ in ilmenite (4 layers) and of $J_{\beta\beta}$ in hematite (2 layers) are known, the modulation in the mixed state is unknown. Therefore, we use a random distribution of ferromagnetic (75%) and antiferromagnetic (25%) links.

The simulations were performed on a 648-cell superlattice using periodic boundary conditions. Fe(II) and Ti(IV) cations were ordered according to the ilmenite $R\bar{3}$ symmetry and 20% were replaced with Fe(III) at random to generate the composition of the investigated solid solution. The thermalization was performed by single-site updates and the system was allowed to thermalize for 1000 cycles per site.

Fig. 4 shows magnetization curves simulated using the described model. As seen in the figure, at $T = 0$ magnetization jumps occur after field reversal and the strongest jumps are near $m = 0$, similar to the experimental curves. With increasing temperature the effects disappear. In addition, observation of the spin-structure during the simulations show that the major moment-rotation during a single jump takes place at the Fe-rich sublattices (see inset to Fig. 4).

Finally, we conclude that the magnetic structure in the presented mixed-spin oxide at low-temperature is partitioned layer-wise by exchange and superexchange interactions. Strong coupling within Fe-rich sublattices leads to a collective rotation of their magnetic moment in an external field, which generates magnetization jumps. Moreover, these observations demonstrate how the layered structure of the $R\bar{3}$ symmetry imparts a collective behavior to this quasi-stochastic system above the percolation threshold.

The authors would like to thank E. Fischer for his assistance in the sample preparation process. This research was supported by the Swiss National Science Foundation Grant No. 200021-121844.

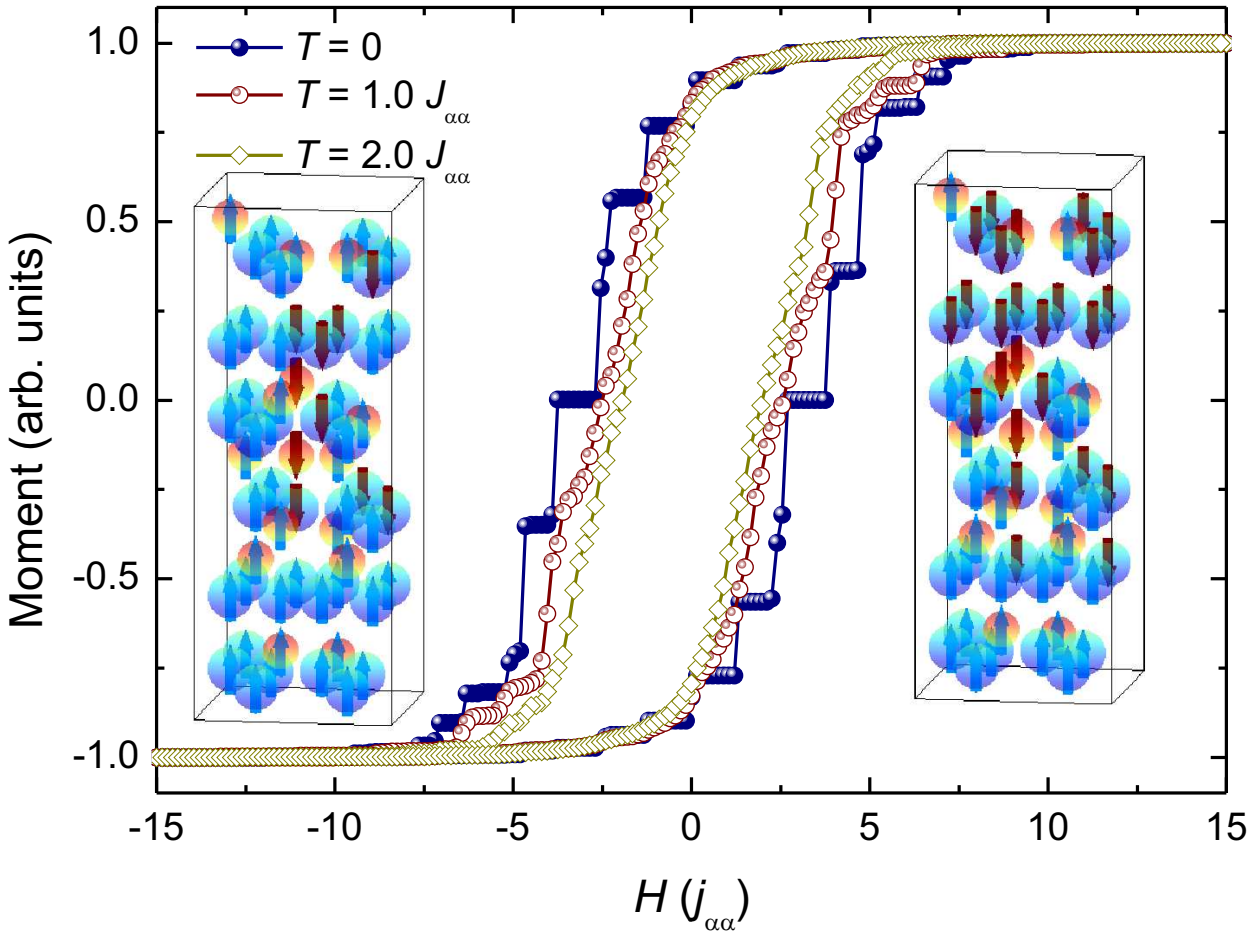

FIG. 4. MC simulation of a magnetization loop at $T = 0$, $T = 1.0\ J_{\alpha\alpha}$, and $T = 2.0\ J_{\alpha\alpha}$. The insets show a portion of the structure before (left) and after (right) a jump of the magnetic moment during the MC simulation at $T = 0$.

* Corresponding author. Email: michalis.charilaou@erdw.ethz.ch

[1] C. A. M. Mulder, A. J. van Duyneveldt, and J. A. Mydosh, Phys. Rev. B **23**, 1384 (1981).

[2] D. Chowdhury and A. Mookerjee, Phys. Rep. **114**, 1 (1984).

[3] K. Binder and A. P. Young, Rev. Mod. Phys. **58**, 801 (1986).

[4] K.H. Fischer and J. A. Hertz, *Spin Glasses*, Cambridge University Press (1991).

[5] J. A. Mydosh, *Spin Glasses: An Experimental Introduction*. Taylor and Francis, London, 1993.

[6] P. W. Anderson, Phys. Rev. **102**, 1008 (1956).

[7] S. Kirkpatrick, C. D. Gelatt, Jr., and M. P. Vecchi, Science **220**, 671 (1983).

[8] G. Aeppli and P. Chandra, Science **275**, 177 (1997).

[9] J. Villain, Z. Phys. B **33**, 31 (1979).

[10] B. Martínez, A. Labarta, R. Rodríguez-Solá, and X. Obradors, Phys. Rev. B **50**, 15779 (1994).

[11] A. P. Ramirez, B. S. Shastry, A. Hayashi, J. J. Krajewski, D. A. Huse, and R. J. Cava, Phys. Rev. Lett. **89**, 067202-1 (2002).

[12] M. E. Zhitomirsky, A. Honecker, and O. A. Petrenko, Phys. Rev. Lett. **85**, 3269 (2000).

[13] Y. K. Tsui, C. A. Burns, J. Snyder, and P. Schiffer, Phys. Rev. Lett. **82**, 3532 (1999).

[14] J. R. L. de Almeida and D. J. Thouless, J. Phys. A: Math. Gen. **11**, 983 (1978).

[15] A. Zheludev, E. Ressouche, I. Tsukada, T. Masuda, and K. Uchinokura, Phys. Rev. B **65**, 174416 (2002).

[16] Y. Suzuki, M. P. Sarachik, E. M. Chudnovsky, S. McHugh, R. Gonzalez-Rubio, Nurit Avraham, Y. Myasoedov, E. Zeldov, H. Shtrikman, N. E. Chakov, and G. Christou, Phys. Rev. Lett. **95**, 147201 (2005).

[17] D. S. Rana and S. K. Malik, Phys. Rev. B **74**, 052407 (2006).

[18] S. McHugh, R. Jaafar, M. P. Sarachik, Y. Myasoedov, A. Finkler, E. Zeldov, R. Bagai, and G. Christou, Phys. Rev. B **80**, 024403 (2009).

[19] N. Marcano, J. C. Gómez Sal, J. I. Espeso, J. M. De Teresa, P. A. Algarabel, C. Paulsen, and J. R. Iglesias, Phys. Rev. Lett. **98**, 166406 (2007).

[20] J. R. Iglesias, J. I. Espeso, N. Marcano, and J. C. Gómez Sal, Phys. Rev. B **79**, 195128 (2009).

[21] S. Nishihara, W. Doi, H. Ishibashi, Y. Hosokoshi, X.-M. Ren, and S. Mori, J. Appl. Phys. **107**, 09A504 (2010).

[22] G. Alejandro, L. B. Steren, A. Caneiro, J. Cartes, E. E. Vogel, and P. Vargas, Phys. Rev. B **73**, 054427 (2006).

[23] Y. Ishikawa, M. Arai, N. Saito, M. Kohgi, and H. Takei, J. Magn. Magn. Mater. **31**, 1381 (1983).

[24] Y. Ishikawa, N. Saito, M. Arai, Y. Watanabe, and H. Takei, J. Phys. Soc. Jpn. **54**, 312 (1985).

[25] R. J. Harrison, S. A. T. Redfern, and R. I. Smith, Am. Mineral. **85**, 194 (2000).

[26] B. P. Burton, P. Robinson, S. A. McEnroe, K. Fabian, and T. B. Ballaran, Am. Mineral. **93**, 1260 (2008).

[27] R. J. Harrison, Geochem. Geophy. Geosy. **10**, Q02Z02 (2009).

[28] M. Charilaou, J. F. Löffler, and A. U. Gehring, Geophys. J. Int. **185**, 647 (2011).

[29] M. Charilaou, J. F. Löffler, and A. U. Gehring, Phys. Rev. B (in press) (2011).

[30] A. U. Gehring, H. Fischer, E. Schill, J. Granwehr, and J. Luster, Geophys. J. Int. **169**, 917 (2007).

[31] A. U. Gehring, G. Mastrogiacomo, H. Fischer, P. G. Weidler, E. Müller, and J. Luster, J. Magn. Magn. Mater. **320**, 3307 (2008).

[32] C. Rüdt, P. J. Jensen, A. Scherz, J. Lindner, P. Poulopoulos, and K. Baberschke, Phys. Rev. B **69**, 014419 (2004).

[33] L. Navarrete, J. Dou, D. M. Allen, R. Schad, P. Padmini, P. Kale, and R.K. Pandey, J. Am. Ceram. Soc. **89**, 1601 (2006).

[34] H. Kato, M. Yamada, H. Yamauchi, H. Hiroyoshi, H. Takei, and H. Watanabe, J. Phys. Soc. Jpn. **51**, 1769 (1982).